

## SMALL-SCALE $H\alpha$ DYNAMIC FEATURES SUPPORTED BY CHROMOSPHERIC MAGNETIC RECONNECTION

SANGWOO LEE<sup>1</sup>, HONG SIK YUN<sup>1</sup>, JONGCHUL CHAE<sup>2</sup>, AND PHILIP R. GOODE<sup>3</sup>

<sup>1</sup>Astronomy Program, SEES, Seoul National University, San 56-1, Shilim Dong, Kwanak Gu, Seoul, 151-742, Korea

*E-mail: leesw@astro.snu.ac.kr*

<sup>2</sup>Department of Astronomy and Space Science, Chungnam National University, Daejeon 305-764, Korea

<sup>3</sup>Big Bear Solar Observatory, NJIT, 40386 North Shore Lane, Big Bear City, CA 92314, USA

### ABSTRACT

In the present study, we have investigated morphology and evolution of small-scale  $H\alpha$  dynamic features on the quiet sun by analyzing video magnetograms and high resolution  $H\alpha$  images simultaneously taken for 5 hours at Big Bear Solar Observatory on April 18, 1997. From comparisons between time sequential longitudinal magnetograms and  $H\alpha$  images covering  $150'' \times 150''$ , several small-scale  $H\alpha$  dynamic features have been observed at a site of magnetic flux cancellation. A close relationship between such features and cancelling magnetic fluxes has been revealed temporarily and spatially. Our results support that material injection by chromospheric magnetic reconnection may be essential in supporting numerous small-scale  $H\alpha$  dynamical absorption features, being in line with recent observational studies showing that material injection by chromospheric magnetic reconnection is essential for the formation of solar filaments.

*Key words* : small-scale  $H\alpha$  dynamic features, chromospheric magnetic reconnection

### I. INTRODUCTION

Magnetic flux cancellation followed by magnetic reconnection has been regarded as a necessary condition of filament formation (e.g., Martin 1998; Tandberg-Hanssen 1995). According to earlier  $H\alpha$  and magnetic observations, the convergence of opposite polarity fields towards their common boundary has always been observed before the filament formation (Litvinenko & Martin 1999; Gaizauskas et al. 1997). Therefore, the role of canceling magnetic fields has been considered to be an essential element in theoretical modeling of the filament magnetic field structure (Martens & Zwaan 2001; DeVore & Antiochos 2000; van Ballegoijen et al. 2000; Galsgaard & Longbottom 1999; Litvinenko 1999; Kuperus 1996; Priest et al. 1994, 1996; van Ballegoijen & Martens 1989, 1990). Besides those large filaments, plenty of small-scale  $H\alpha$  absorption features are often observed throughout the solar surface even in quiet regions. It has become easier to observe and analyze such features due to increased spatial and temporal resolution in  $H\alpha$  and magnetogram observations. Therefore, it would be interesting to find out how such small-scale features are related with nearby small-scale magnetic elements, especially with flux cancellation of small magnetic elements, as described above.

The small-scale  $H\alpha$  absorption features are sometimes called ‘mini-filaments’ due to their appearance similar to ‘normal’ filaments. The ‘mini-filaments’ have been first observed and mentioned in literature

by Moore et al. (1977) and Labonte (1979). Labonte (1979) described such events as ‘macrospicules’ both from limb and disk observations in  $H\alpha$ . More detailed study on ‘mini-filaments’ has been done by Hermans & Martin (1986). Recently, the relation between mini-filaments and magnetic fields was studied by Wang et al. (2000) and Zhang et al. (2000) based on the observations performed at Big Bear Solar Observatory. From a careful examination of a sample of 88 events, Wang et al. (2000) concluded that mini-filaments also lie along a magnetic neutral line and spatially correlated with canceling magnetic features. But the description of the cancelling magnetic features was limited since they focused mainly on their morphological evolution seen in  $H\alpha$ . A more detailed study on the magnetic evolution associated with small-scale  $H\alpha$  dynamic features (they called macrospicules) was done by Zhang et al. (2000). They concluded that macrospicules are triggered by interaction between intranetwork and network elements or among several network elements.

The purpose of this study is to further investigate morphological and evolutionary relationship of  $H\alpha$  dynamic features with magnetic fields, based on simultaneous  $H\alpha$  and magnetic observations of a quiet region with high spatial and time resolution. Our observation supports that small-scale  $H\alpha$  dynamic features are strongly associated with flux cancellation both spatially and temporarily.

### II. OBSERVATION AND DATA REDUCTION

The present observation was performed to obtain time sequential  $H\alpha$  images and video magnetograms

---

*Corresponding Author: S. Lee*

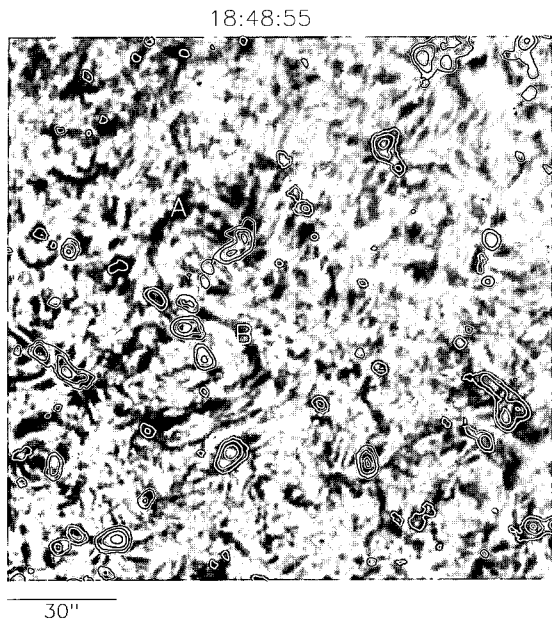


**Fig. 1.**— The  $H\alpha$  filtergram overlapped with the corresponding longitudinal magnetogram, showing the positions A and B where notable small-scale features occurred. White contours correspond to positive polarity and black to negative polarity. The spatial scale is  $150'' \times 150''$ , and the contour levels are  $[-80, -40, -20, -10, 10, 20, 40, 80(\text{Gauss})]$ .

of a solar quiet region at Big Bear Solar Observatory on April 18, 1997. The  $H\alpha$  images were taken with the OSL CCD camera attached to the  $26''$  reflector. The video magnetograms were obtained with the  $10''$  refractor in Fe I  $6103\text{\AA}$  line. A quiet region at disk center was selected as the target, which is free from the geometric projection effect. The total duration of the observation was about 5 hours excluding the last two hours of cloudy data.

An  $H\alpha$  image was recorded every 30 seconds and a magnetogram was taken approximately every 3 minutes. The  $H\alpha$  filter was usually tuned to the line center most time. The magnetograms were taken by integrating 4096 frames. The spatial scale was calibrated by momentarily drifting the telescope to the west and the north by  $50''$  for  $H\alpha$  images and by  $100''$  for magnetograms. After trimming the bad portions near the outer boundary of both images, the field of view of  $H\alpha$  images was found to be  $224'' \times 201''$ . The field of view of magnetograms was found to be  $382'' \times 271''$ , which is larger than that of  $H\alpha$  images. Although the duration of our observation was originally 7.5 hours, we selected the first 5-hour data due to bad seeing in later hours.

We have aligned all the images by shifting each image by the amount of the displacement determined by applying the technique of cross-correlation. Many  $H\alpha$  images suffered from large-scale non-uniformity. This

non-uniform pattern was modeled by a two-dimensional low degree polynomial fit to each image and was subtracted from the original image.

### III. RESULTS

From now on, we will concentrate on a  $150'' \times 150''$  region of our interest near the central part, and will show the details of  $H\alpha$  dynamic features. For this purpose, we have selected 275  $H\alpha$  images and 72 magnetograms of good quality covering the same period of almost 5 hours. The initial investigation of the temporal evolution was done based on a MPEG movie that was constructed from these images.

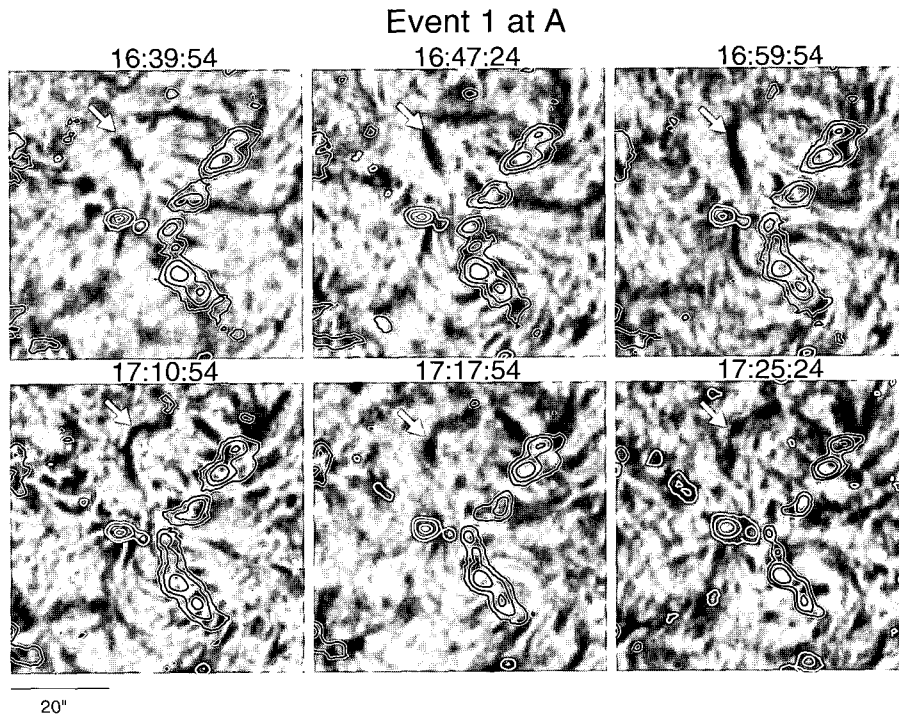
Figure 1 shows an  $H\alpha$  snapshot image displaying a few  $H\alpha$  features which we will study in detail. We observed four of this kind of features during our observing run, three of which occurred at position A and one at B. All of these features were associated with canceling magnetic features as seen in the overlapped magnetogram.

#### (a) $H\alpha$ Dynamic Events at Regions A and B

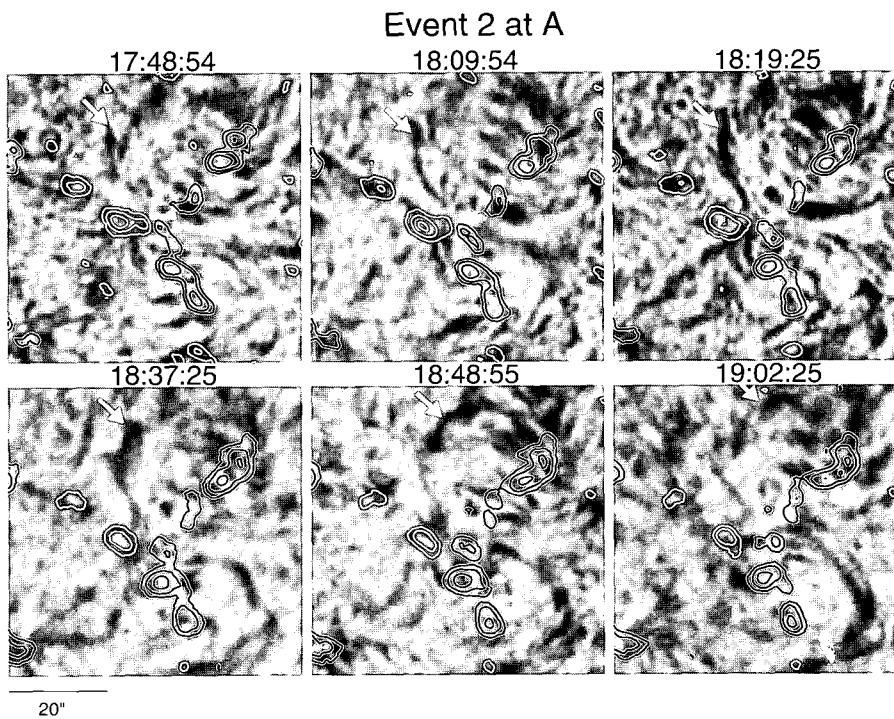
Figure 2 shows the development of the first event at A. It existed from the beginning of our observation, so we do not know how it started. Initially it was a straight absorption feature, but it changed into a curved shape (17:10:54), lasting until 17:25:24. The length of this feature is measured to be  $20''$ . Note that this feature was located at the site of colliding opposite magnetic polarities at the network boundary, suggesting the flux cancellation. But because of the lack of observation in the beginning phase, we can not determine whether flux cancellation really occurred or not.

Figure 3 shows the development of the second feature at A. It started at 17:48:54 and lasted about an hour. It moved along almost the same curved trajectory as the first feature did. The length of this feature is measured to be  $23''$ . This looks like a magnetic loop, as inferred from the corresponding opposite magnetic polarities of the two footpoints. This feature is associated with strong flux concentration and is located at chromospheric network boundary. It has been ejected from a magnetic element of negative polarity with a curved and closed shape. A careful examination of the magnetograms represented in contours in Figure 3 reveals that the opposite magnetic fluxes located at the center of the frames decreased during this event (for example, compare between 18:19:25 and 18:37:25).

Figure 4 shows the third feature at A that started at 19:13:28 and lasted about an hour. Although this one shows a spiky or surge-like shape unlike the two previous ones, its evolutionary behavior, lifetime and location do not differ from others. The magnetic maps in Figure 4 clearly indicates that this feature also occurred during magnetic flux cancellation. Therefore, it can be concluded that a series of small-scale  $H\alpha$  events of the similar property repeatedly occurred at the same



**Fig. 2.**— The H $\alpha$  images showing the temporal evolution of the first H $\alpha$  absorption feature at position A. The FOV is  $60'' \times 60''$  and the contour levels are same as in Fig. 1. Note the morphological evolution of the feature indicated by white arrow.



**Fig. 3.**— The H $\alpha$  images showing the temporal evolution of the second H $\alpha$  absorption feature at position A. The FOV is  $60'' \times 60''$  and the contour levels are same as in Fig. 1. Note the morphological evolution of the feature indicated by white arrow.

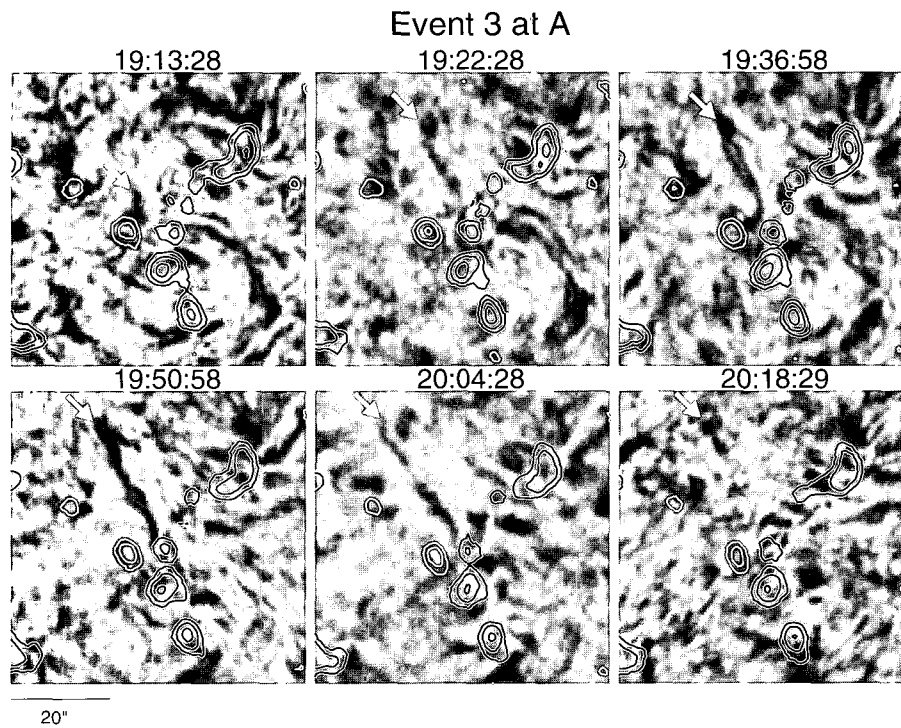


**Fig. 4.**— The  $H\alpha$  images showing the temporal evolution of the third  $H\alpha$  absorption feature at position A. The FOV is  $60'' \times 60''$  and the contour levels are same as in Fig. 1. Note the morphological evolution of the feature indicated by white arrow.

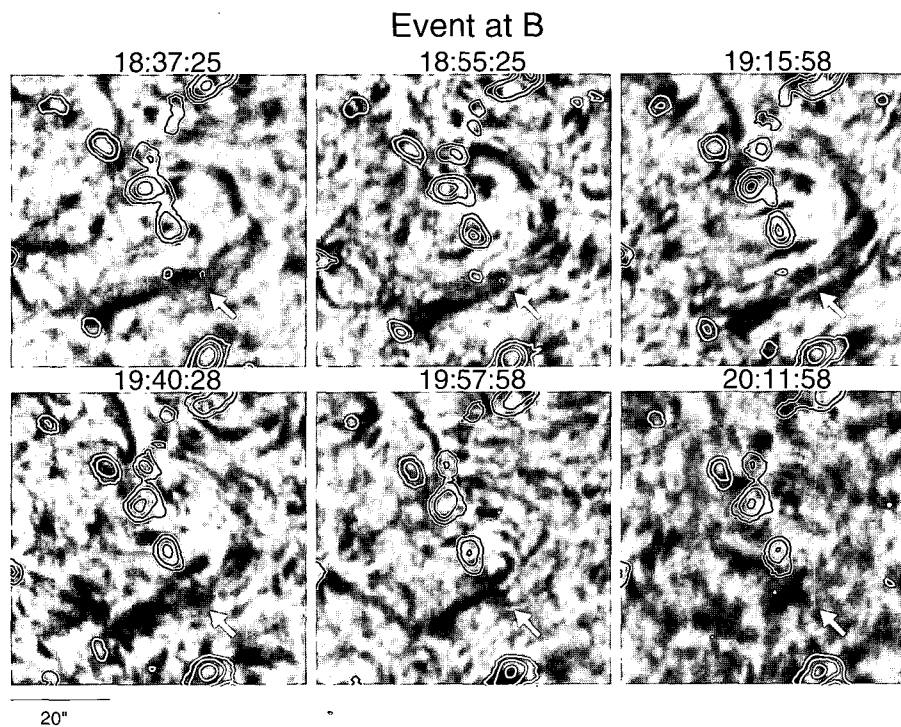


**Fig. 5.**— The  $H\alpha$  images showing the temporal evolution of the  $H\alpha$  absorption feature at position B. The FOV is  $60'' \times 60''$  and the contour levels are same as in Fig. 1. Note the morphological evolution of the feature indicated by white arrow.

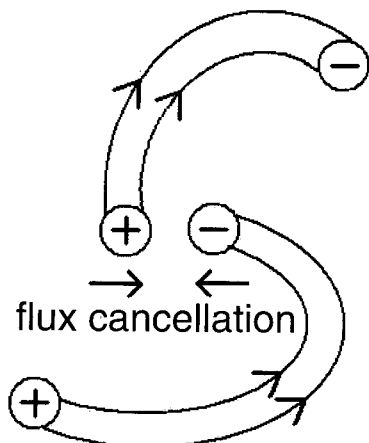


**Fig. 6.**— Schematic diagram of the magnetic field around the features A and B.

location during flux cancellation. This finding is consistent with the previous studies that reported the association of flux cancellation with a series of discrete events such as explosive events (Chae et al. 1998a) and H $\alpha$  upflow events (Chae et al. 1998b).

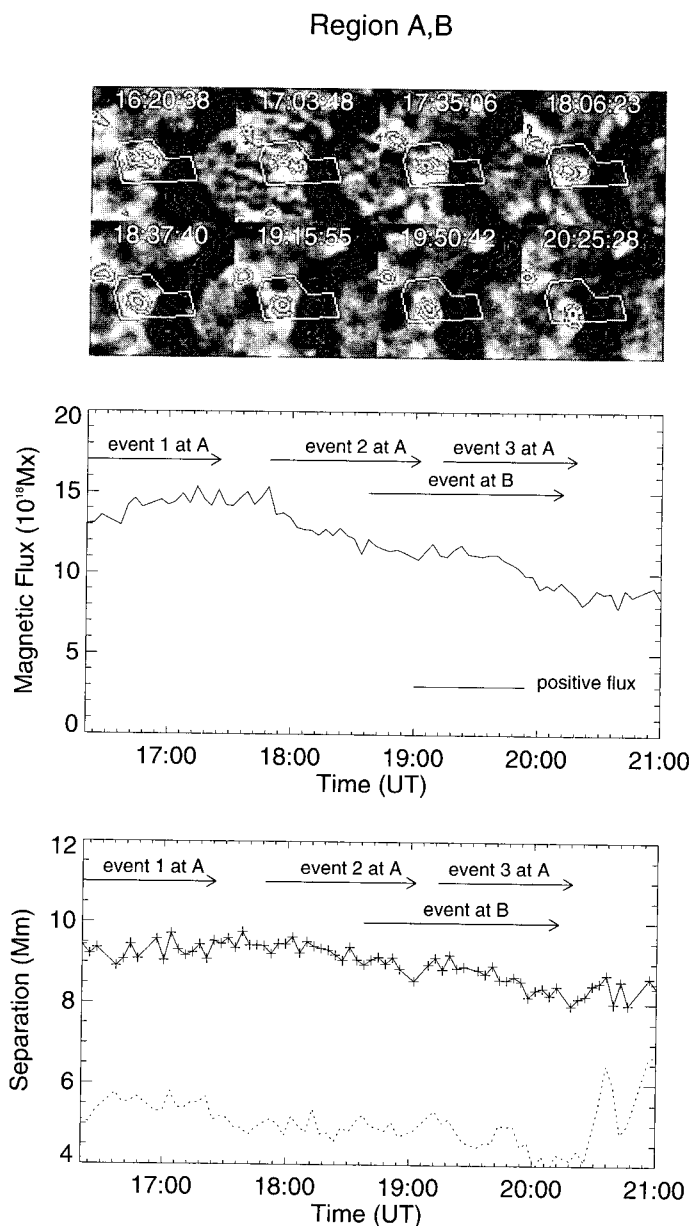
Figure 5 shows the evolution of a feature at B. It started at 18:37:25 and lasted about 1.5 hours. It has the largest length of 60'' among the observed features. It looks like the ones on A except that it follows a different trajectory. A comparison with the magnetogram indicates that the trajectory connects between two opposite polarities, suggesting a magnetic loop structure. Thus, at least two magnetic loops have been identified that are rooted near the site of flux cancellation: one at A and the other B. Moreover, the footpoints of these loops at the flux cancellation site have opposite polarities. Therefore, the flux cancellation and the H $\alpha$  dynamic events may be a consequence of the interaction of the two loops.

Figure 6 shows a possible configuration that illustrates the two interacting loops. The interaction might have led to magnetic flux cancellation, playing an important role in the occurrences of those small-scale features. This feature at B can also be regarded to have the same physical origin (magnetic reconnection) as the previous ones at A, inferring from its location, morphology and evolutionary behavior.

### (b) Parameters of Flux Cancellation

Our comparison between H $\alpha$  and magnetogram observations has indicated that the dynamic H $\alpha$  features originated from chromospheric material injection at the flux cancellation site.

Figure 7 shows the time variation of the magnetic flux at the site of flux cancellation (A and B). The upper and middle panels show that the positive polarity suffered substantial decrease of magnetic flux. The decreasing rate of magnetic flux is measured to be



**Fig. 7.**— *Top*: a time sequence of magnetograms showing the temporal variation of magnetic fluxes in a region of  $40'' \times 40''$  where the three H $\alpha$  absorption features at A and B appeared. Flux densities of  $\pm 6, 12, 24, 48$  G and so on are shown in gray-scale discontinuities. *Middle*: the time variation of the integrated magnetic flux for positive polarity. *Bottom*: the time variation of the separated distance between the center of positive and negative polarity (solid line). The spatial extent of negative flux along the interface between the two polarities is also estimated with the method developed by Chae et al. (2002) and drawn with dashed line.

$4.3 \times 10^{18} \text{ Mx h}^{-1}$  for positive polarity. The negative polarity, which belongs to rather strong magnetic elements of network boundary, showed no substantial flux decrease. Therefore, only the positive polarity has been taken into account. Most importantly, it can be obviously seen that the duration of the feature corresponds to the early phase of flux cancellation. Therefore, the formation of this feature is clearly associated with magnetic flux cancellation resulting from magnetic reconnection of two opposite polarities.

We have measured several other parameters of flux cancellation in addition to flux cancellation rates. The converging speed toward the polarity reversal boundary has been calculated by measuring temporal variation of the separation between positive and negative polarity. The mean approaching speed is estimated to be  $0.10 \text{ km s}^{-1}$  at A and B, respectively. The contact length between two opposite polarities are also measured with methods developed by Chae et al.(2002) to be 5 Mm at this location. Now, the specific cancellation rate  $r$  is calculated (flux cancellation rate divided by contact length) to be  $2.6 \times 10^6 \text{ G cm s}^{-1}$ . These measurements are compatible with those measured from small-scale flux cancellations by Chae et al.(2002). The average rate of flux cancellation of photospheric magnetic elements has also been measured by Litvinenko and Martin(1999) to be order of  $10^{19} \text{ Mx h}^{-1}$ , higher than our measurement. Considering the fact that they focused on magnetic elements near active region, our measurement is fairly comparable to their result.

#### IV. DISCUSSION

Simultaneous observations of  $H\alpha$  and longitudinal magnetic fields of a quiet region performed with high spatial and temporal resolution have clearly demonstrated that the small-scale  $H\alpha$  absorption features are closely associated with magnetic flux cancellation process. The observed features commonly have short lifetime of 1~1.5 hour and small spatial extent of 20~60". They tend to recur at the same location. The observed features look like surges or mass injections to magnetic loop.

They may be identified with macrospicules previously reported by Labonte (1979), Wang et al. (2000) and Zhang et al. (2000). Their appearance seems quite different from so called mini-filaments (miniatures of large-scale filaments) previously reported by Moore et al. (1977), Hermans and Martin (1986) and Wang et al. (2000). Despite their morphological difference, those two kind of features share many similar characteristics such as lifetime, size, and strong association with flux cancellation. Therefore, we are not sure whether making an arbitrary distinction between them is physically meaningful or not.

The connectivities of magnetic elements as seen in  $H\alpha$  image imply that magnetic fields are highly non-potential. Such a configuration might be related to chromospheric magnetic reconnection as manifest in

flux cancellation. Non-potentiality of magnetic fields appears to be important in the activity of small-scale magnetic activities in the quiet Sun as well as in active regions (Woodard & Chae 1999).

Our results support that material injection by chromospheric magnetic reconnection at the quiet sun network is essential for supporting small-scale  $H\alpha$  dynamic features. This finding is in line with recent observational and theoretical studies showing that material injection by chromospheric magnetic reconnection is essential for the formation of filaments (Chae et al. 2001; Gaizauskas et al. 2001; Litvinenko & Martin 1999; Priest et al. 1996). The flux cancellation rates, mean approaching speeds and contact lengths between two opposite polarities measured in this study are compatible with the results from small magnetic poles previously measured by Chae et al. (2002). If such examples could be found to happen frequently throughout the solar surface, it may imply that chromospheric magnetic reconnection is quite common, and plays a potential role of dynamically supporting the chromosphere by supplying mass.

#### ACKNOWLEDGEMENTS

Upon his retirement, S. Lee and J. Chae would like to express their sincere thanks to Professor Yun who has kindly supervised them. They wish to keep close communication and cooperation with him even after his retirement. This work is supported in part by the Korea-US Cooperative Science Program (KOSEF 995-0200-002-2, NSF INT-98-16267) and by the BK21 project of the Korean Government.

#### REFERENCES

- Chae, J., Wang, H., Lee, C. Y., Goode, P., & Schüle, U. 1998a, Photospheric magnetic field changes associated with transition region explosive events, *ApJ*, 497, L109
- Chae, J., Wang, H., Lee, C. Y., Goode, P., & Schüle, U. 1998b, Chromospheric upflow events associated with transition region explosive events, *ApJ*, 504, L123
- Chae, J., Wang, H., Qiu, J., Goode, P. R., Strous, L., & Yun, H. S. 2001, The formation of a prominence in active region NOAA 8668. I. SOHO/MDI observations of magnetic field evolution, *ApJ*, 560, 476
- Chae, J., Moon, Y.-J., Wang, H., & Yun, H. S. 2002, Flux cancellation rates and converging speeds of cancelling magnetic features, *Sol. Phys.*, 207, 73
- DeVore, C. R., & Antiochos, S. K. 2000, Dynamical formation and stability of helical prominence magnetic fields, *ApJ*, 539, 954
- Gaizauskas, V., Zirker, J. B., Sweetland, C., & Kovacs, A. 1997, Formation of a solar filament channel, *ApJ*, 479, 448
- Gaizauskas, V., Mackay, & Harvey, K. L. 2001, Evolution of solar filament channels observed during a

- major poleward surge of photospheric magnetic flux, ApJ, 558, 888
- Galsgaard, K., & Longbottom, A. W. 1999, Formation of solar prominence by flux convergence, ApJ, 510, 444
- Hermans, L. M., & Martin, S. F.:1986, In A. I. Poland (ed.), Small-scale eruptive filaments on the quiet sun, Coronal and Prominence Plasmas, NASA Conf. Publ. 2442
- Kuperus, M. 1996, The double inverse polarity paradigm, Sol. Phys., 169, 349
- Labonte, B. J. 1979, Activity in the quiet sun. I - Observations of macrospicules in H-alpha and D3, Sol. Phys., 61, 283.
- Litvinenko, Y. E. 1999, Photospheric magnetic reconnection and cancelling magnetic features on the sun, ApJ, 515, 435
- Litvinenko, Y. E., & Martin, S. F. 1999, Magnetic reconnection as the cause of a photospheric cancelling feature and mass flows in a filament, Sol. Phys., 190, 45
- Martens, P. C., & Zwaan, C. 2001, Origin and evolution of filament-prominence systems, ApJ, 558, 872
- Martin, S. F. 1998, Conditions for the formation and maintenance of filaments, Sol. Phys., 182, 107
- Moore, R. L., Tang, F., Bohlin, J. D., & Golub, L. 1977, H-alpha macrospicules - Identification with EUV macrospicules and with flares in X-ray bright points, ApJ, 218, 286
- Priest, E. R., Parnell, C. E., & Martin, S. F. 1994, A converging flux model of an X-ray bright point and an associated cancelling magnetic features, ApJ, 427, 459
- Priest, E. R., van Ballegoijen, A. A., & Mackay, D. H. 1996, A model for dextral and sinistral prominences, ApJ, 460, 530
- Tandberg-Hanssen, E. 1995, In The Nature of Solar Prominences, p. 114.
- van Ballegoijen, A. A., & Martens, P. C. H. 1989, Formation and eruption of solar prominences, ApJ, 343, 971
- van Ballegoijen, A. A., & Martens, P. C. H. 1990, Magnetic fields in quiescent prominences, ApJ, 361, 283
- van Ballegoijen, A. A., Priest, E. R., & Mackay, D. H. 2000, Mean field model for the formation of filament channels on the sun, ApJ, 539, 983
- Wang, J., Li, W., Denker, C., Lee, C., Wang, H., Goode, P. R., MacAllister, A., & Martin, S. F. 2000, Mini-filament eruption on the quiet sun. I. Observations at H $\alpha$  central line, ApJ, 530, 1071
- Woodard, M. F., & Chae, J. 1999, Evidence for non-potential magnetic fields in the quiet sun, Sol. Phys., 184, 239
- Zhang, J., Wang, J., Lee, C.-Y., & Wang, H. 2000, Macrospicules observed with H $\alpha$  against the quiet solar disk, Sol. Phys., 194, 59